Ultralow magnetic damping of a common metallic ferromagnetic film

February 1 2021, by Thamarasee Jeewandara

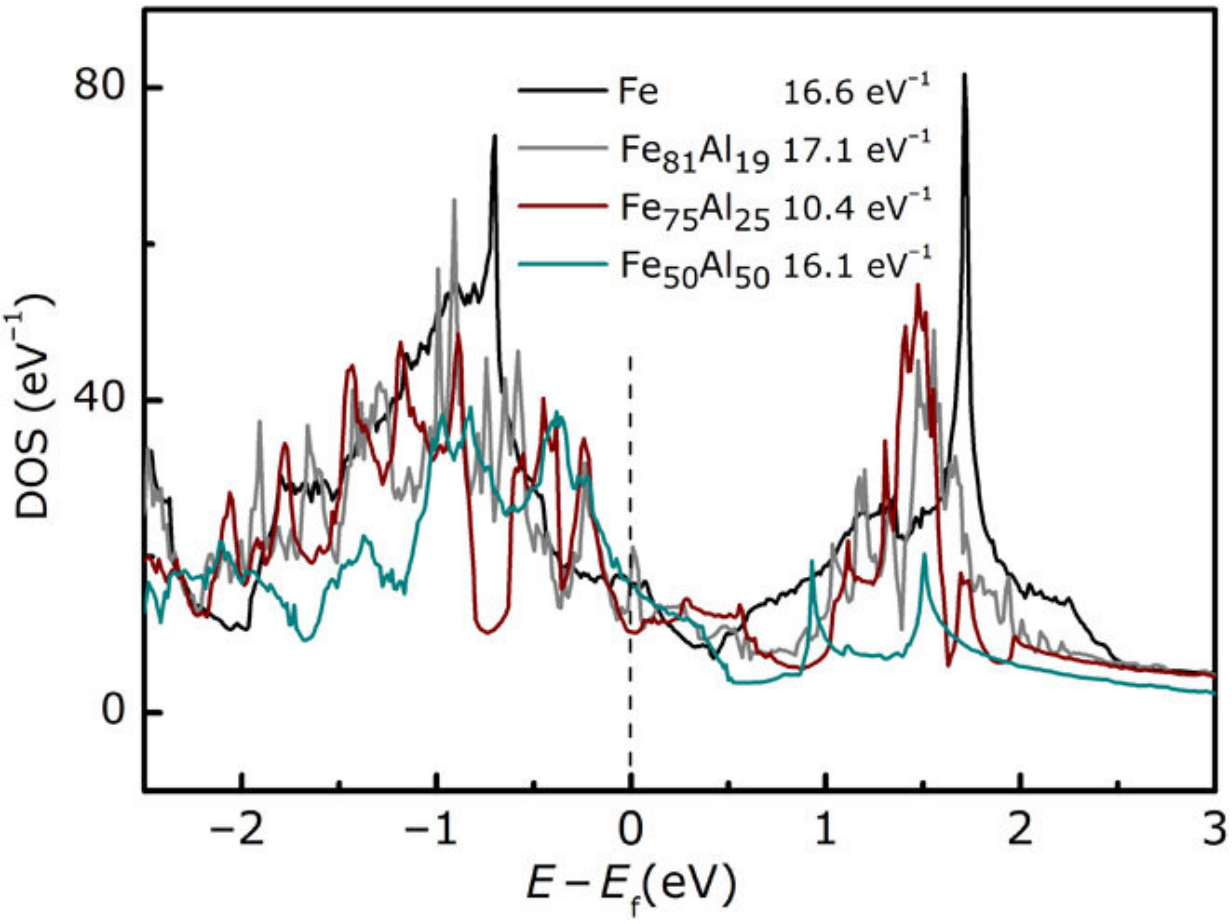

Several calculated representative electron DOS of Fe1−xAlx (x = 0, 19, 25, and 50). Eight bcc unit cells with 16 Fe atoms are used to construct a supercell for pure Fe DOS calculations and for Fe1−xAlx with different concentrations x where Fe on various sites are replaced by Al. The energies are given relative to the Fermi energy, Ef = 5.87 eV, for comparison, and inset numerical values are those of the DOS at the Fermi energy for FeAl with various compositions

labeled. Credit: *Science Advances*, doi: 10.1126/sciadv.abc5053

Ultralow damping is of key importance for spintronic and spin-orbitronic applications in a range of magnetic materials. However, the number of materials that are suited for charge-based spintronic and spin-orbitronic applications are limited due to magnon-electron scattering. To quantitatively calculate the transition metallic ferromagnetic damping, researchers have proposed theoretical approaches including the breathing Fermi surface model (to describe dissipative magnetization dynamics), generalized torque correlation model, scattering theory, and the linear response damping model. In a new report now published on *Science Advances*, Yangping Wei and a team of scientists in science, magnetism and magnetic materials, and chemical engineering in China and Singapore experimentally detailed a damping parameter approaching 1.5 x 10^{-3} for traditional, fundamental iron aluminide (FeAl) soft ferromagnets. The results were comparable to those of 3-D transition metallic ferromagnets based on the principle of minimum electron density of states.

Ultralow magnetic damping

Ultralow magnetic damping can allow to meet the energy and speed requirements of devices for spintronic and spin-orbitronic applications. Ultralow damping can, however, contradict the charge current requirements for most applications since such charge currents can cause high damping due to magnon-electron scattering. Yttrium-iron-garnet (YIG) materials are ferromagnetic insulators with low damping and are good candidates to achieve properties of low-energy consumption and high speed, suited for spintronic devices. Compared to 3-D transition metal ferromagnets, research efforts on the magnetic damping of traditional, fundamental iron aluminide (FeAl) soft ferromagnets, which

possess excellent mechanical and functional properties at a low cost, remain rare. The comparatively low magnetic damping achieved for an FeAl metallic system can make it a promising material for spintronic and spin-orbitronic applications. In this work, Wei et al. examined the electronic structure of $Fe_{1-x}Al_x$ using density functional theory (DFT) calculations conducted with the Vienna Ab initio simulation package (VASP) and the generalized gradient approximation (GGA). The team also grew a high-quality single-crystalline Fe-Al alloy film with a thickness of 20 nm and a 3-nm-thick capping aluminum layer on magnesium oxide (MgO), using molecular beam epitaxy (MBE) and studied the compositional effect of damping on the alloys. The team then used in situ reflection high-energy electron diffraction (RHEED) and high-resolution X-ray diffraction (HRXRD) methods to demonstrate the single domain texture of the FeAl films. Using frequency sweeps with various mixed-magnetic field ferromagnetic resonance (FMR) measurements, Wei et al. found low magnetic damping effects.

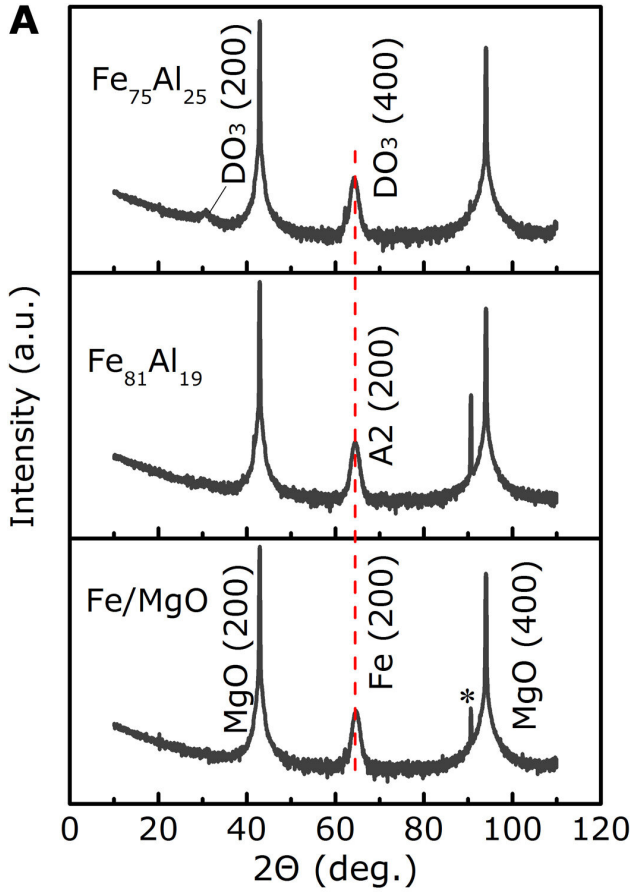
A
Fe75Al25
DO3 (200)
DO3 (400)
Fe81Al19
A2 (200)
Fe/MgO
MgO (200)
Fe (200)
*
MgO (400)
Intensity (a.u.)
0 20 40 60 80 100 120
2Θ (deg.)

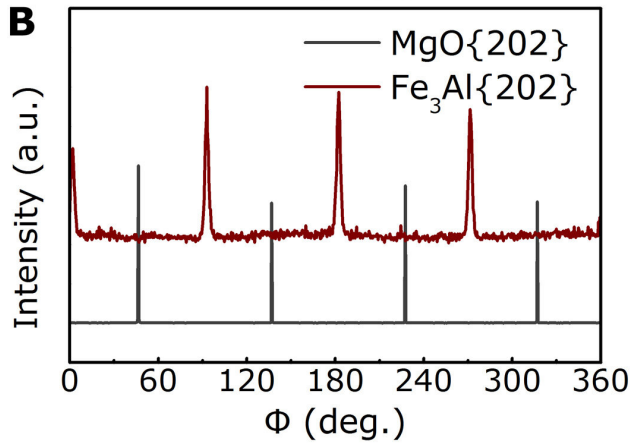
B
MgO{202}
Fe3Al{202}
Intensity (a.u.)
0 60 120 180 240 300 360
Φ (deg.)

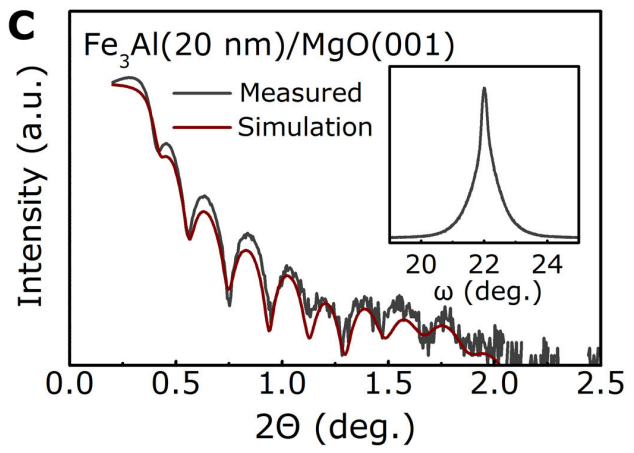
C
Fe3Al(20 nm)/MgO(001)
Measured
Simulation
20 22 24
ω (deg.)
Intensity (a.u.)
0.0 0.5 1.0 1.5 2.0 2.5
2Θ (deg.)

High-resolution x-ray diffractometry and reflectometry of Fe1−xAlx alloy films on MgO. (A) Longitudinal HRXRD ω-2Θ scans of the Fe1−xAlx alloy films with various Al concentrations grown on the MgO(100) substrate. The asterisked peak is the reflection of Al2O3 substrate for loading samples during testing. The slight changes in the diffraction angle of the samples account for distortion of the lattice, and the lattice changes are indicated by the comparison to the red dashed line. For Fe3Al, an obvious new diffraction peak (200) appears at 30.7o. a.u., arbitrary units. (B) Azimuthal HRXRD Φ scans of the Fe3Al{202} and MgO{202} planes. For the Fe3Al/MgO scan, four reflections at 45o intervals are observed, indicating an in-plane fourfold symmetry and a relative 45o rotation epitaxial growth of the Fe3Al films on the MgO substrate. (C) High-resolution x-ray reflectometry scans of the Fe3Al /MgO films where a corresponding fit (brown) gives a thickness of 20 nm for Fe3Al and a roughness of 0.7 and 0.4 nm for MgO and Fe3Al, respectively. Inset: HRXRD rocking curve of the Fe3Al (202) peak gives a full width at half-maximum of 0.49°. Credit: *Science Advances*, doi: 10.1126/sciadv.abc5053

Density functional theory calculations and the characterization of crystalline structures

During the study, Wei et al. used eight body-centered cubic (bcc) unit cells with 16 iron atoms to construct a supercell to calculate pure iron density of states (DOS). The $Fe_{1-x}Al_x$ contained different concentrations of x, where iron on various sites were replaced by aluminum atoms. The team obtained several representative DOS for the FeAl alloy and found them to exhibit a minimum at the Fermi level at aluminum concentrations of 25%. The team then set the chamber pressure of the custom-designed molecular beam epitaxy for sample growth at a favorable rate to fabricate high quality, single-crystalline $Fe_{1-x}Al_x$ alloy films under nonequilibrium conditions. The RHEED (reflection high-

energy electron diffraction) patterns showed the attainment of a pure single-orientation relationship. The team assessed the dependence of the fine crystal structure of the $Fe_{1-x}Al_x$ films on the concentration of aluminum using HRXRD (high-resolution X-ray diffraction). As the aluminum concentration increased, they noted the formation of a solid solution of aluminum in iron. The team then assessed the thickness and roughness of the films using an X-ray reflectometry scan.

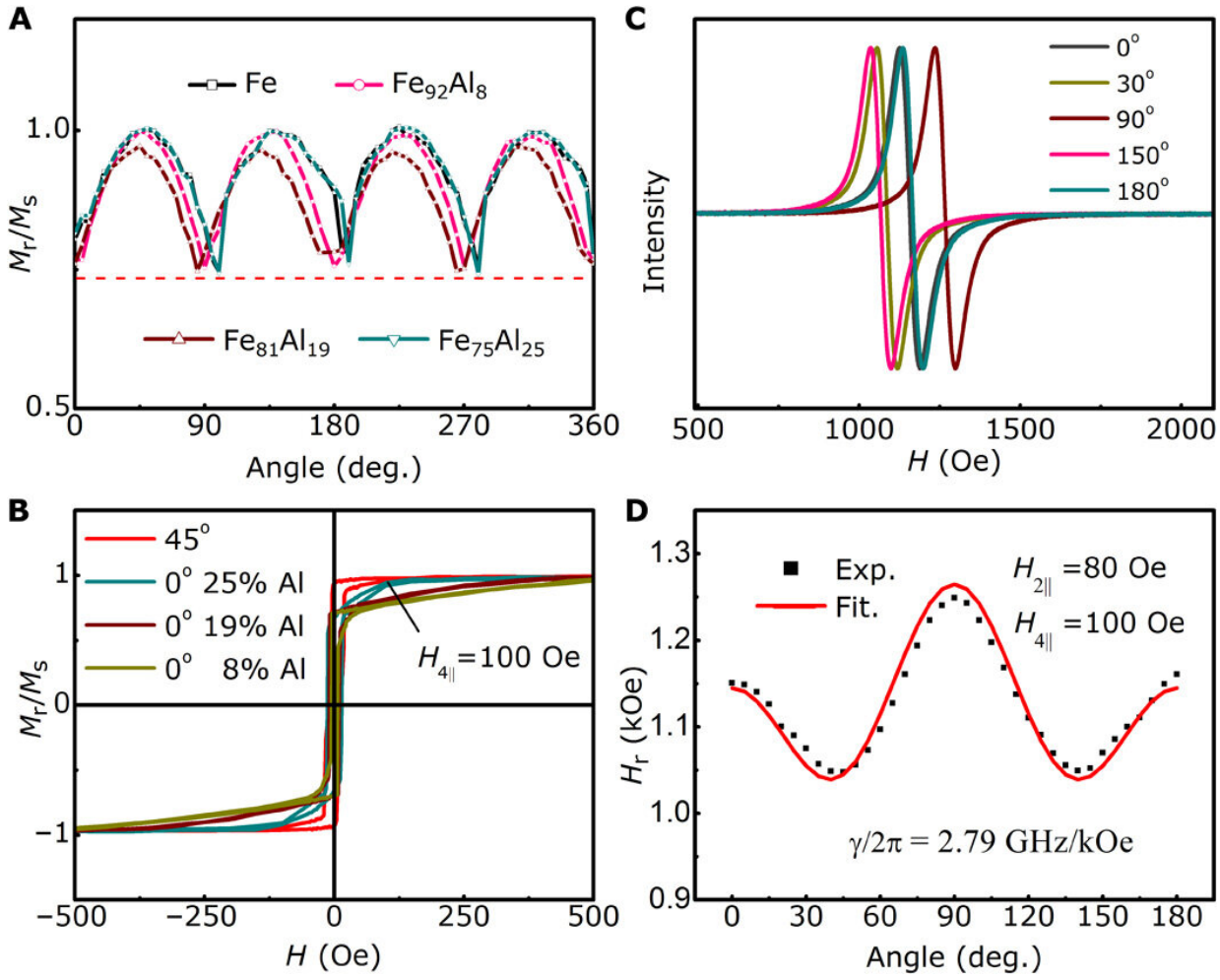

The angular dependence of the remanent magnetization and ferromagnetic resonance (FMR) and the dependence of magnetocrystalline anisotropy on Al content. (A) 0° is the starting point along the MgO[010] direction in the measured angle-remanent curves showing second minimum Mr that indicates the

hard magnetization direction corresponding to the Fe1−xAlx [011], and Mr reaches its maximum value at 45o corresponding to the easy magnetization direction along the Fe1−xAlx [010]. The dashed line is a guide for identifying the first and second minimum Mr. (B) Magnetic hysteresis loops along the easy and hard magnetization axes of the Fe1−xAlx showing the dependence on Al concentration. The saturation field along the easy magnetization direction labeled with 45o remains constant and the hard magnetization direction labeled with 0o decreases as the Al concentrations increases, indicating that the magnetocrystalline anisotropy of Fe1−xAlx becomes weaker with increasing Al content. (C) Derivative FMR absorption spectra for Fe3Al from 0o (corresponding to the MgO[010] direction) to 180o at a microwave frequency of 9.4 GHz. (D) Series of resonant fields fitted by the experimental data for the extraction of H2∥ and H4∥. Credit: *Science Advances*, doi: 10.1126/sciadv.abc5053

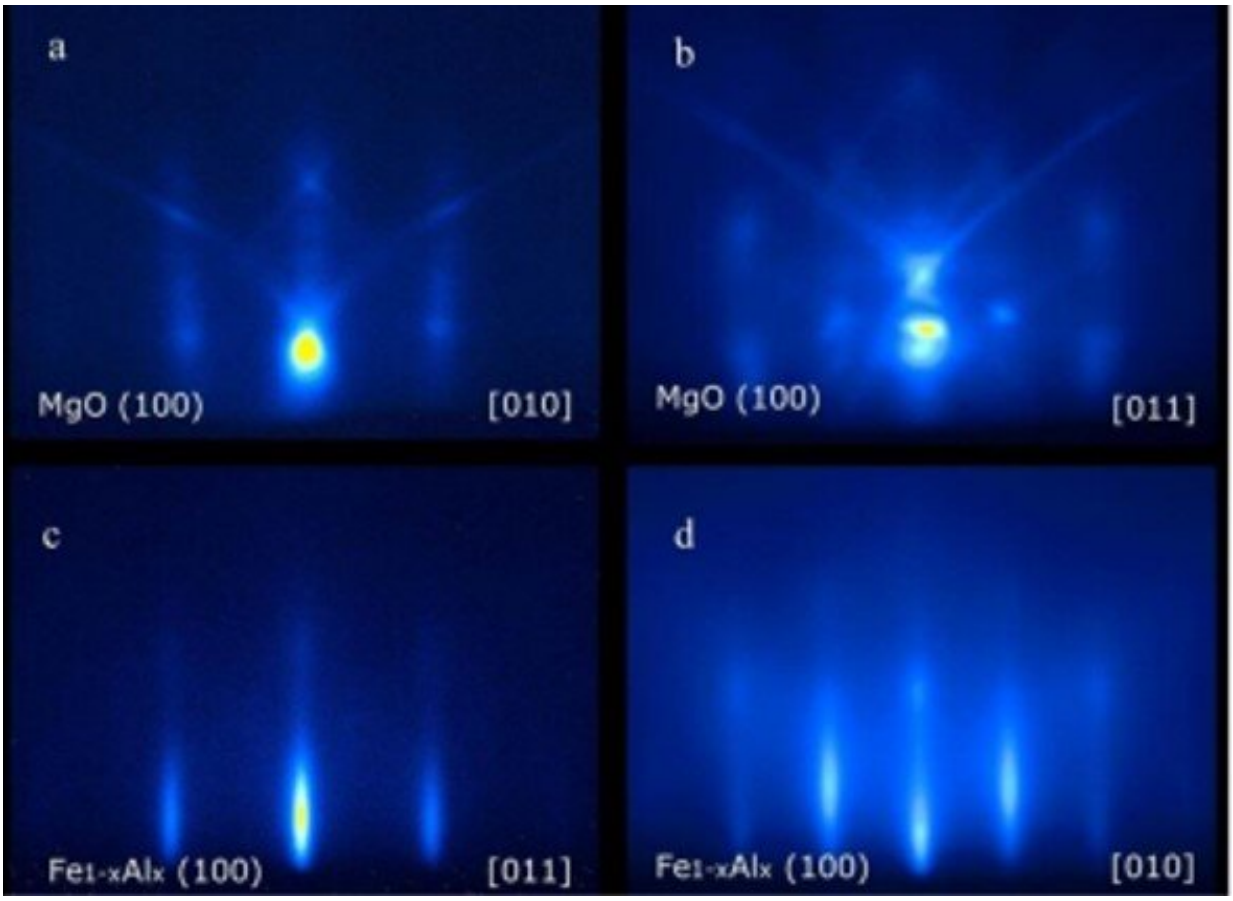

RHEED patterns of (a) (100)-oriented MgO, the electron beam is along the in-plane direction of [010] and (b) (100)-oriented MgO, the electron beam is along the in-plane direction of [011]. (c, d) RHEED patterns of Fe1-xAlx film grown on it, respectively. Credit: *Science Advances*, doi: 10.1126/sciadv.abc5053

Characterization of basic magnetization

To explain the easy and hard magnetizing directions of the iron-aluminum films, Wei et al. measured angle-remnant curves using a vibrating sample magnetometer (VSM). As the aluminum concentration varied from zero to 25%, the saturation magnetization of the sample changed. Meanwhile, in the hard magnetization direction, as the saturation field decreased with increasing aluminum concentration, the magnetocrystalline anisotropy became weaker. To determine the value of the magnetic anisotropy of the material, the team used angular-dependent ferromagnetic resonance measurements. The team then measured the damping torque, known as Gilbert damping in the setup, where its direction was given by the vector product of the magnetization and its time derivative. For instance, the resulting Gilbert damping parameter (α) for $Fe_{75}Al_{25}$ films was comparable to values described in previous studies.

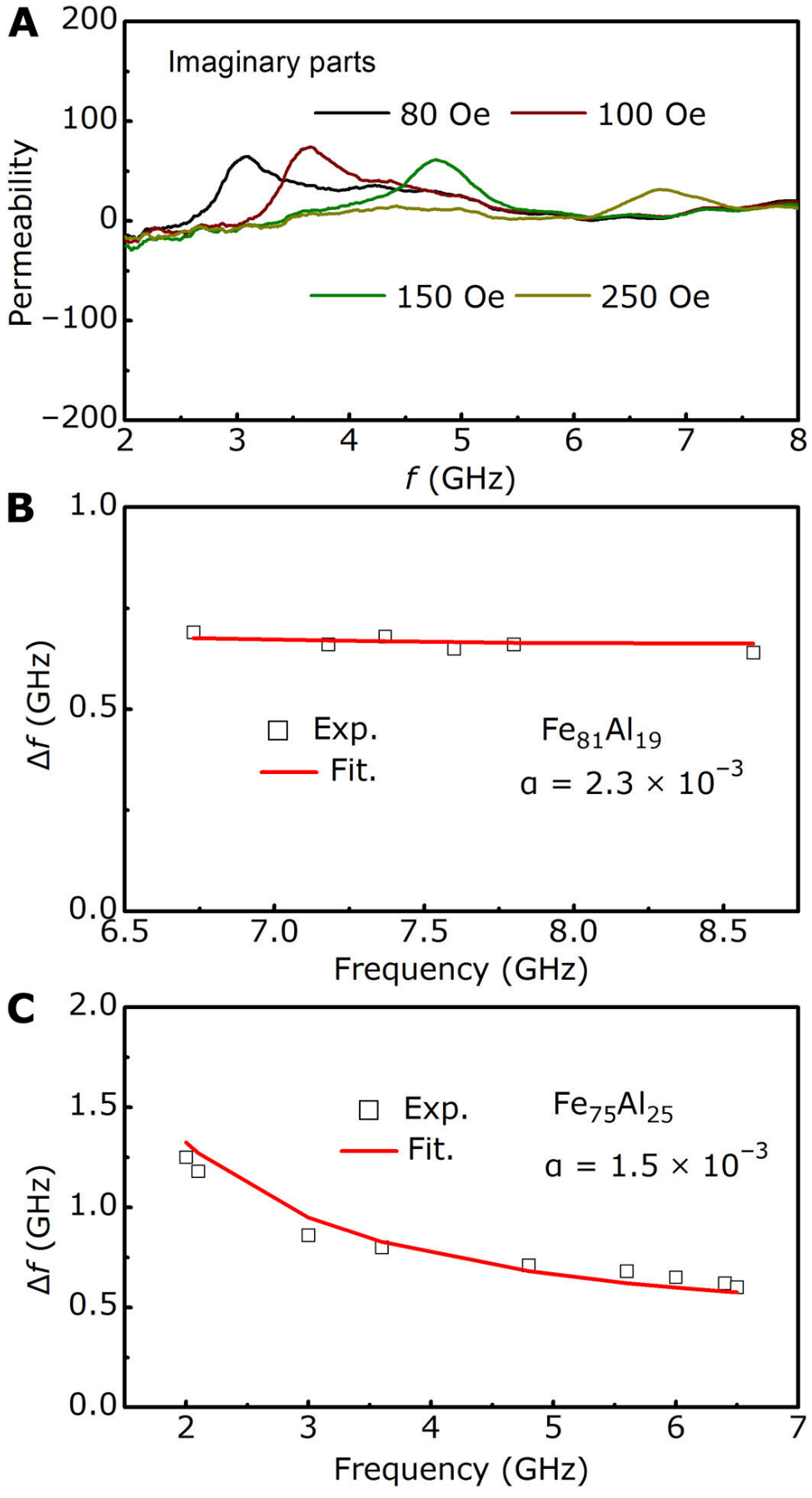
A
Imaginary parts
80 Oe
100 Oe
150 Oe
250 Oe
Permeability
f (GHz)
B
Exp.
Fit.
Fe81Al19
α = 2.3 × 10−3
Δf (GHz)
Frequency (GHz)
C
Exp.
Fit.
Fe75Al25
α = 1.5 × 10−3
Δf (GHz)
Frequency (GHz)

Determination of Gilbert damping. (A) The resonance frequency shifts higher as external field increases, and the frequency width dependence of the frequency was obtained by frequency sweeps for the Fe75Al25 films. (B and C) Corresponding frequency width dependence of the frequency for the Fe75Al25 and Fe81Al19 films. Gilbert damping parameter values were fitted by an equation derived in the study and were $\alpha = 1.5 \times 10{-}3$ and $\alpha = 2.3 \times 10{-}3$, respectively. Credit: *Science Advances*, doi: 10.1126/sciadv.abc5053

In this way, Yangping Wei and colleagues observed ultralow magnetic damping of 1.5 x 10^{-3} in traditional FeAl crystalline ferromagnets at an aluminum concentration of 25%. The work offers a new opportunity to select low-cost materials not limited to 3-D transition metallic elements for spintronic and spin-orbitronic applications. The team obtained these novel results on the basis of the principle of minimum density of states proposed previously. The results further verified magnetic damping to be proportional to the density of states at the Fermi level in the same alloy. The work enables a new approach to screen materials for spintronic and spin-orbitronic applications and expand the method to a broader range of low-damping materials.

More information: Wei Y. et al. Ultralow magnetic damping of a common metallic ferromagnetic film, *Science Advances*, DOI: 10.1126/sciadv.abc5053

Schoen M. A. W. et al. Ultra-low magnetic damping of a metallic ferromagnet, *Nature Physics*, doi.org/10.1038/nphys3770

Gilmore K. et al. Identification of the dominant precession-damping mechanism in Fe, Co, and Ni by first-principles calculations. *Physical Review Letters*, doi.org/10.1103/PhysRevLett.99.027204